THE CASIMIR–POLDER INTERACTION BETWEEN TWO NEUTRONS AND POSSIBLE RELEVANCE TO TETRANEUTRON STATES*

M.S. Hussein[a,b,c], J.F. Babb[d], R. Higa[c]

[a]Instituto Tecnológico de Aeronáutica, DCTA
12228-900 São José dos Campos, SP, Brazil
[b]Instituto de Estudos Avançados, Universidade de São Paulo
C.P. 72012, 05508-970 São Paulo-SP, Brazil
[c]Instituto de Física, Universidade de São Paulo
R. do Matão 1371, 05508-090 São Paulo, SP, Brazil
[d]ITAMP, Harvard-Smithsonian Center for Astrophysics
MS 14, 60 Garden St., Cambridge, MA 02138, USA

(Received August 10, 2017)

We present a summary of our recent publication concerning the derivation of the extended Casimir–Polder (C–P) dispersive interaction between two neutrons. Dynamical polarizations of the neutrons, recently derived within Chiral Effective Theory, are used for the purpose. An account of the higher frequency/energy behavior of these entities related to the opening of one-pion production channel and the excitation of the Δ resonance are taken into consideration in our derivation of the C–P interaction. The neutron–neutron system in free space is treated in details so are the neutron–wall and the wall–neutron–wall systems. The case of tetraneutron (a 4-neutron system) in a resonant state is then briefly considered. The $4n$ C–P interaction is evaluated to assess its potential relevance to the ongoing debate concerning the nature of the tetraneutron.

DOI:10.5506/APhysPolB.48.1837

1. Introduction

It is by now a given fact that hadrons are bound entities of fractionally charged quarks and the ensuing effects of this picture results in their electric and magnetic polarizabilities. The long-distance strong interaction between neutrons arise from exchanges of quarks and gluons in colorless

* Presented by M.S. Hussein at the 2nd Jagiellonian Symposium on Fundamental and Applied Subatomic Physics, Kraków, Poland, June 3–11, 2017.

states (bosons) driven mainly by the underlying chiral symmetry of quantum chromodynamics (QCD). The electromagnetic interactions between well-separated neutrons arise from the Casimir–Polder (C–P) effect related to the dipole polarizability [1–3]. Knowing the C–P interaction involving neutrons is important from the practical point of view as it has relevance in ultracold neutron physics and, in particular, in the understanding of the working of neutron confining bottles. In this contribution, we give a summary of our recent publication on the subject and also comment on the tetraneutron.

2. C–P interaction between two neutrons

Recently, we have investigated the neutron–neutron dispersive Casimir–Polder interaction between two neutrons [4]. In that work, we assessed the importance of internal excitation of the neutron and pion production on the dynamic polarizabilities. We present in this section our results for the n–n, C–P interaction.

As shown by Feinberg and Sucher [5], the asymptotic ($r \sim \infty$) long-distance electromagnetic interaction between two neutrons is given by the Casimir–Polder potential

$$\begin{aligned} V^{\infty}_{\mathrm{CP},nn}(r) &= -\frac{\hbar c}{4\pi r^7}\left[23\left(\alpha_n^2+\beta_n^2\right)-14\alpha_n\beta_n\right]+\mathcal{O}\left(r^{-9}\right) \\ &= V^{*}_{\mathrm{CP},nn}(r)+\mathcal{O}\left(r^{-9}\right), \end{aligned} \tag{1}$$

with the notation of V^{*}_{CP} meaning the static limit of the nucleon dynamic polarizabilities. Bernabéu and Tarrach, on the other hand, derived the analogous long-range potential between a proton and a neutron [2]

$$\begin{aligned} V^{\infty}_{\mathrm{CP},pn}(r) &= \hbar c\,\alpha_0\left[-\frac{\alpha_n}{2r^4}+\frac{1}{4\pi c M_p r^5}(11\alpha_n+5\beta_n)+\mathcal{O}\left(r^{-7}\right)\right] \\ &= V^{*}_{\mathrm{CP},pn}(r)+\mathcal{O}\left(r^{-7}\right), \end{aligned} \tag{2}$$

where M_p is the proton mass and $\alpha_0 = e^2/4\pi \sim 1/137$ is the electromagnetic fine structure constant. It exhibits the leading repulsive r^{-5} term from the polarizabilities of the neutron induced by the charge of the proton, followed by the r^{-7} interaction bilinear in the two nucleon polarizabilities.

In Ref. [4], we improved the above description by considering the frequency dependence on the so-called dynamical dipole polarizabilities. At distances large enough that exchange forces can be neglected, the Casimir–Polder interaction between two neutrons follows from [3, 5]

$$V_{\mathrm{CP},ij}(r) = -\frac{\alpha_0}{\pi r^6} I_{ij}(r)\,, \tag{3}$$

where

$$I_{ij}(r) = \int_0^\infty \mathrm{d}\omega e^{-2\alpha_0\omega r}\Big\{ [\alpha_i(i\omega)\alpha_j(i\omega) + \beta_i(i\omega)\beta_j(i\omega)]\, P_{\mathrm{E}}(\alpha_0\omega r) + [\alpha_i(i\omega)\beta_j(i\omega) + \beta_i(i\omega)\alpha_j(i\omega)]\, P_{\mathrm{M}}(\alpha_0\omega r)\Big\},$$

$$P_{\mathrm{E}}(x) = x^4 + 2x^3 + 5x^2 + 6x + 3\,, \qquad P_{\mathrm{M}}(x) = -\left(x^4 + 2x^3 + x^2\right)\,, \quad (4)$$

and $\alpha_i(\omega)$ and $\beta_i(\omega)$, respectively, are the dynamic electric and magnetic dipole polarizability of particle i, and similarly for particle j.

Theoretical and experimental studies on the nucleon polarizabilities have a long tradition in hadron physics, as they unravel important information about the internal structure of hadrons (for a review, see [6]). Low-energy analyses with photon energies up to the excitation of the Δ resonance were performed within the effective theory of QCD in such regime, namely, chiral effective field theory [6–10]. The energy dependence of the neutron dipole polarizabilities $\alpha_n(\omega)$, $\beta_n(\omega)$ involve long expressions and integrals that are far from simple. Given this, in [4] we proposed a parametrization with a simpler form that takes into account the one-pion production cusp and the Δ resonance contribution

$$\alpha_n(\omega) = \frac{\alpha_n(0)\sqrt{(M_\pi + a_1)(2M_n + a_2)}(0.2a_2)^2}{\sqrt{\left(\sqrt{|M_\pi^2 - \omega^2|} + a_1\right)\left(\sqrt{|4M_n^2 - \omega^2|} + a_2\right)}\,[|\omega|^2 + (0.2a_2)^2]}\,, \quad (5)$$

$$\beta_n(\omega) = \frac{\beta_n(0) - b_1^2\omega^2 + b_2^3\mathrm{Re}(\omega)}{\left(\omega^2 - \omega_\Delta^2\right)^2 + \left|\omega^2\Gamma_\Delta^2\right|} \quad (6)$$

with fitting parameters a_1, a_2, b_1, b_2, ω_Δ, and Γ_Δ. The parameter a_1 is formally a higher order effect, but is important to match the correct pion production threshold, which controls the low-energy behavior of $\alpha_n(\omega)$ [7]. The square roots in Eq. (5) are attempts to incorporate the pion production threshold behavior above which α_n develops an imaginary part. The parameters ω_Δ and Γ_Δ, respectively, are quite close to the n–Δ mass splitting and the resonance width as exhibited in Table 1 of [4]. These specific forms also assume the smooth and asymptotically decreasing behavior of α_n and β_n at imaginary frequencies, which are expected from analyticity of the Compton S-matrix and are used in the construction of our Casimir–Polder potentials.

We fit Eqs. (5) and (6) to the covariant formulation of baryon chiral effective field theory (CB-χEFT) of Lensky, McGovern, and Pascalutsa [10], which takes proper account of the nucleon recoil corrections to all orders.

For $M_n = 938.919$ MeV and letting M_π be a free parameter, we obtain $M_\pi = 134.051$ MeV, which is fairly close to the neutral pion mass (134.98 MeV). The remaining parameters are given in [4]. The parametrizations yield dynamic polarizabilities, shown in Figs. 1 and 2, that visibly describe well the results of [10] and remain well within the comparatively large theoretical uncertainties [6, 10]. We also checked that our results are in qualitative agreement with chiral EFT results at imaginary frequencies up to iM_π [4].

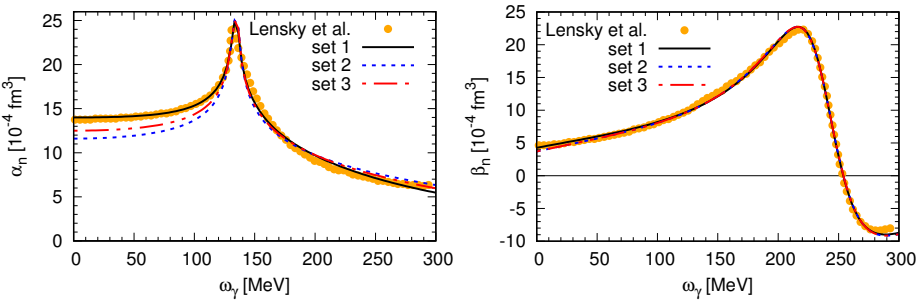

Figure 1. (Color online) Dynamic electric (left) and magnetic (right) polarizabilities, as functions of the photon energy ω_γ. The gray/yellow circles are the CB-χEFT results of Lensky *et al.* [10], while sets 1, 2, and 3 correspond to our parametrizations using the numbers specified in [4].

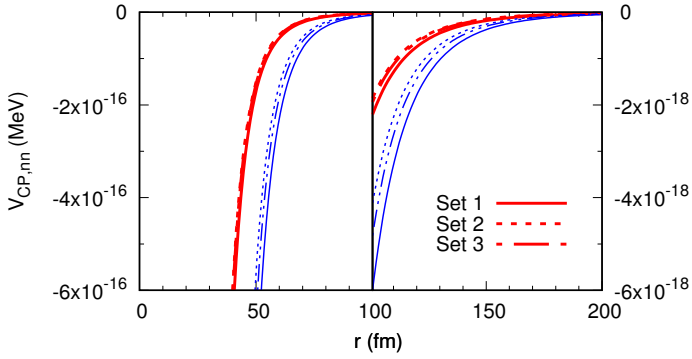

Figure 2. (Color online) C–P interaction for two neutrons, as a function of the separation distance r. The bold red and thin blue lines correspond to the use of dynamical and static dipole polarizabilities, respectively.

From our parametrizations (5), (6), we obtain the neutron–neutron C–P interaction via Eqs. (3) and (4). The results are given in Fig. 2 as functions of the separation distance. The bold red curves correspond to $V_{\mathrm{CP},nn}(r)$ given by the dynamic polarizabilities previously shown, while the thin blue curves correspond to the static limit $\alpha_n(\omega)$, $\beta_n(\omega) \to \alpha_n(0)$, $\beta_n(0)$. It is clear

from Fig. 3 that the effect of dynamical polarizabilities is to decrease the magnitude of the potential up to distances as far as 200 fm. The expected long-distance limit of Eq. (1) can be inspected in Fig. 3. We use parameters from set 3, which illustrates well the qualitative behavior of the other sets. In the dashed (red) curve we multiplied the C–P potential by $s\,r^6$, where $s = 100$ fm to fit in the figure. The long-dashed (blue) and solid black lines, respectively, are the dynamic and static polarizabilities versions of $V_{\mathrm{CP},nn}$ (the latter indicated by $V^*_{\mathrm{CP},nn}$ in the figure), multiplied by r^7. The thin solid (red) line is the arctan parametrization [11] commonly used in atomic physics (see, for example, Ref. [12]) to make the transition from the $1/r^6$ van der Waals to the asymptotic $1/r^7$ Casimir–Polder behavior [13].

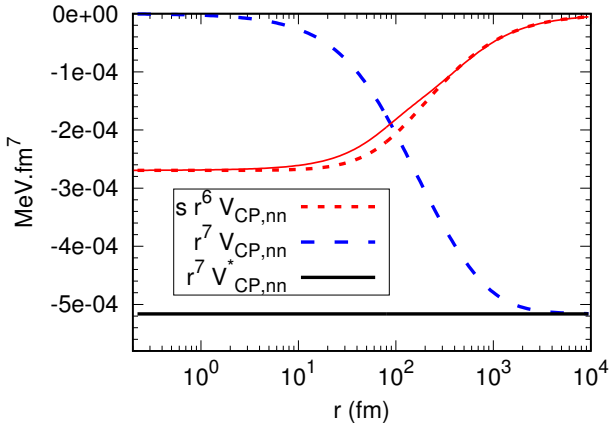

Figure 3. (Color online) The neutron–neutron C–P interaction as a function of the separation distance r, multiplied by $s\,r^6$ (dashed (red) line, with $s = 100$ fm) and r^7 (long-dashed (blue) line). The solid black line is the C–P potential from the static limit of the dipole polarizabilities, multiplied by r^7.

The dashed (red) curve evidences the $1/r^6$ behavior at small distances up to ≈ 20 fm — a region that is dominated by energies larger than used to set our parametrizations (5), (6). This can be checked via the dominance of the exponential factor in Eq. (4): $r \lesssim 20$ fm involves photon energies larger than $(2\alpha_0 \times 20\ \mathrm{fm})^{-1} \sim 670$ MeV. The Delta resonance starts contributing at about $(2\alpha_0\omega_\Delta)^{-1} \sim 50$ fm, mostly via $\beta_n(\omega)$ which is numerically of $\sim 10\%$. Our results can, therefore, be considered valid for distances beyond 50 fm. The same reasoning applies to the contribution of the pion production threshold, at around 100 fm. The expected asymptotic behavior (1) is only reached for $r \gtrsim 10^3$ fm, dominated by dynamic polarizabilities in the region of $\omega_\gamma \lesssim 10$ MeV [4].

In Ref. [4], we have also calculated the neutron–wall C–P interaction and the wall–neutron–wall interaction. For completeness, we show the results in Fig. 4 below and further details can be found in [4].

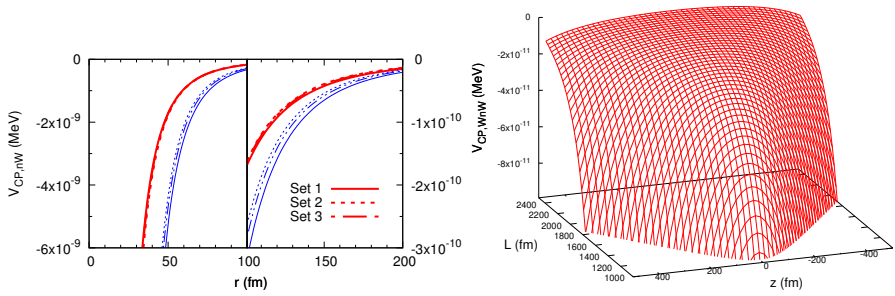

Figure 4. Left panel: C–P interaction for a neutron and a wall as a function of the separation distance r. Notation is the same as in Fig. 2. Right panel: C–P interaction for a neutron between two walls as a function of the neutron position from the midpoint z and the separation between the two walls L.

3. The C–P interaction among three and four neutrons

As we have discussed in Section 2, the C–P interaction between two neutrons is not very sensitive to the high frequency dispersive response of the neutron connected with the opening of the one-pion production channel and the excitation of the $3/2^+\Delta$ resonance. Nevertheless, the overall C–P interaction associated with the usual dipole–dipole dispersive force is appreciable and detectable through careful analysis of low-energy n–n scattering.

3.1. The 3n C–P interaction

It is certainly of interest to investigate the C–P interaction among three, four and more neutrons. The usual approach to this few and many-body system through the introduction of a mean field is not appropriate here [15]. The non-additive dispersive C–P potentials for three and four neutrons can be read off from this paper, and we give here the final results appropriate for a given geometry. For an equilateral triangular configuration of three neutrons with sides of length r, the general result of [15] would give

$$V_{3n}^{\rm CP}(r) = \frac{2^4 \times 79}{3^5}\frac{\hbar c}{\pi}\frac{\alpha_n^3}{r^{10}} = 1.73\frac{\hbar c}{\pi}\frac{\alpha_n^3}{r^{10}}\,, \tag{7}$$

while the linear configuration n–n–n with the inner n–n separation being $r/2$ gives

$$V_{3n}^{\rm CP}(r) = -186\frac{\hbar c}{\pi}\frac{\alpha_n^3}{r^{10}}\,. \tag{8}$$

The prediction of [15] for three neutral molecules as extended to neutrons in this paper shows that the geometry plays a central role. The C–P interaction is repulsive in the triangular case, while it is attractive in the linear case. This is in contrast to the two-neutron C–P interaction which is universally attractive.

3.2. The 4n C–P interaction and its potential relevance to the tetraneutron

We turn now to the C–P interaction in the case of a tetramolecule as derived by [15] and as applied here for the 4-neutron system in the spatial configuration of a regular tetrahedron, shown schematically in Fig. 5, with a neutron at points A, B, C, and D, and segments AB, AC, AD, BC, BD, and CD of length r,

$$V_{4n}^{\mathrm{CP}}(r) = -\frac{3 \times 41 \times 2689}{2^{15}} \frac{\hbar c}{\pi} \frac{\alpha_n^4}{r^{13}} = -633 \frac{\hbar c}{\pi} \frac{\alpha_n^4}{r^{13}}\,, \tag{9}$$

which is universally attractive.

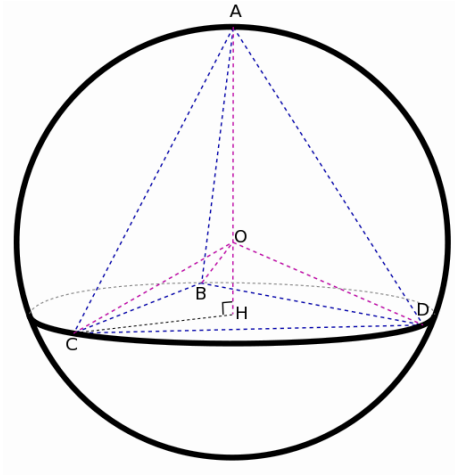

Figure 5. A tetrahedron with its circumsphere [14].

To summarize, with the value of the electric polarizability $\alpha_n = 12.6 \times 10^{-4}$ fm^3, we have the following results:

1. For the equilateral triangle,

$$V_{3n}^{\mathrm{CP}}(r) = 2.12 \times 10^{-7} \frac{1}{r^{10}}\ [\mathrm{MeV}]\,. \tag{10}$$

2. For the linear chain, n–n–n with the n–n separation $r/2$

$$V_{3n}^{\mathrm{CP}}(r) = -2.28 \times 10^{-5} \frac{1}{r^{10}} \ [\mathrm{MeV}] . \tag{11}$$

3. For the regular tetrahedron configuration of edge length r, we have

$$V_{4n}^{\mathrm{CP}}(r) = -1.55 \times 10^{-9} \frac{1}{r^{13}} \ [\mathrm{MeV}] . \tag{12}$$

In all the equations above, r is in femtometer.

It is known that there is no bound dineutron. This fact became important in so far as the recent production of Borromean nuclei, such as ^{6}He and ^{11}Li, where the structure is understood as a bound core plus two neutrons. None of the two fragment subsystems are bound, *e.g.*, $^{4}\mathrm{He} + n = {}^{5}\mathrm{He}$, $n+n$ are unbound, and similarly for ^{11}Li considered as a stable core, ^{9}Li are bound to two neutrons; with $^{9}\mathrm{Li} + n = {}^{10}\mathrm{Li}$ and $n + n = 2n$ being unbound.

There are also no bound or observable resonant trineutron states. The cause for this is the Fermi nature of the neutron and the corresponding Pauli exclusion principle.

The quest for bound tetraneutrons was started back in the early sixties [16, 17], where the possible existence of the bound tetraneutron in the reaction $^{4}\mathrm{He}(\gamma,\pi^{+})^{4}\mathrm{H} \to {}^{3}\mathrm{H} + n$ was claimed. This result was challenged by [18] through the study of the byproducts of the induced and spontaneous fission of uranium and californium. They obtained negative results.

The search for tetraneutrons was revived with the advent of secondary beams of very neutron rich unstable nuclei such as ^{8}He, ^{11}Li, ^{14}Be and ^{15}B. Reference [19] studied the reactions of these exotic nuclei with a carbon target, and detected tetraneutrons in the elastic breakup reaction $^{14}\mathrm{Be} + {}^{12}\mathrm{C} \to 4n + {}^{10}\mathrm{Be} + {}^{12}\mathrm{C}$. These results posed a great challenge to nuclear structure theory, as Pieper [20] has pointed out. Pieper used the most realistic nuclear Hamiltonian at the time which predicts successfully many properties of the nucleus, and could not find a bound tetraneutron system.

In 2016, Kisamori *et al.* [21] studied the reaction ^{4}He (^{8}He, ^{8}Be) and found a resonant tetraneutron state in the missing mass spectrum. This energy of the tetraneutron resonance was found to be $E_{\mathrm{R}} = 0.83 \pm 0.63(\mathrm{statistical}) \mp 1.25(\mathrm{systematic})$ MeV above the threshold of four-neutron decay. The width of this resonance, Γ_{R}, was found to be 2.6 MeV (Full Width at Half Maximum). Clearly, $\Gamma_{\mathrm{R}} > 2E_{\mathrm{R}}$. Three theoretical papers [22–24] contested the existence of a tetraneuron resonance as it would require the inclusion in the four-body description a strong three-nucleon force which would have an undesirable consequence on the other properties of the nuclear system. On the other hand, Fossez *et al.* [25] performed a realistic

structure calculation which included the coupling to the continuum a resonant $4n$ state at roughly the same energy of [21], but the width came out to be larger than 3.7 MeV. Since the tetraneutron resonance is a wide resonance in the sense that its width is larger than twice its energy, its decay would deviate appreciably from a simple exponential. The tiny C–P interaction may play a role on the decay and lower the value of the width, though a careful calculation of the influence of the C–P force on the basic nn scattering length would be needed, and with this a reexamination of the $4n$ interaction and decay properties can be assessed. This work is in progress.

4. Conclusions

In this contribution, we have discussed our recent findings about the Casimir–Polder interaction between neutrons. In particular, we assessed the importance of the pion production threshold and the Δ resonance on our dispersive potentials. We also considered the C–P interaction between three and four neutrons. Relevance of our findings about the $4n$ C–P interaction on the decay properties of the recently observed tetraneutron resonance is pointed out. Further work on this last point is required to better pin down the role of the $4n$ C–P interaction.

J.B. is supported in part by the U.S. NSF through a grant for the Institute of Theoretical Atomic, Molecular, and Optical Physics at Harvard University and Smithsonian Astrophysical Observatory. R.H. and M.S.H. are supported in part by the Fundação de Amparo à Pesquisa do Estado de São Paulo (FAPESP). M.S.H. is also supported by the Conselho Nacional de Desenvolvimento Científico e Tecnológico (CNPq) and by the Coordenação de Aperfeiçoamento de Pessoal de Nível Superior (CAPES), through the CAPES/ITA-PVS program.

References

[1] H.B.G. Casimir, D. Polder, *Phys. Rev.* **73**, 360 (1948).

[2] J. Bernabéu, R. Tarrach, *Ann. Phys. (NY)* **102**, 323 (1976).

[3] J.F. Babb, *Adv. At. Mol. Opt. Phys.* **59**, 1 (2010).

[4] J.F. Babb, R. Higa, M.S. Hussein, *Eur. Phys. J. A* **53**, 126 (2017).

[5] G. Feinberg, J. Sucher, *Phys. Rev. A* **2**, 2395 (1970).

[6] F. Hagelstein, R. Miskimen, V. Pascalutsa, *Prog. Part. Nucl. Phys.* **88**, 29 (2016).

[7] R.P. Hildebrandt, H.W. Griesshammer, T.R. Hemmert, B. Pasquini, *Eur. Phys. J. A* **20**, 293 (2004).

[8] R.P. Hildebrandt, Ph.D. Thesis, Technical Univ. München, 2005.
[9] H.W. Griesshammer, J.A. McGovern, D.R. Phillips, G. Feldman, *Prog. Part. Nucl. Phys.* **67**, 841 (2012) [arXiv:1203.6834 [nucl-th]].
[10] V. Lensky, J. McGovern, V. Pascalutsa, *Eur. Phys. J. C* **75**, 604 (2015).
[11] M. O'Carroll, J. Sucher, *Phys. Rev.* **187**, 85 (1969).
[12] H. Friedrich, G. Jacoby, C.G. Meister, *Phys. Rev. A* **65**, 032902 (2002).
[13] L.G. Arnold, *Phys. Lett. B* **44**, 401 (1973).
[14] URL: https://commons.wikimedia.org/wiki/File:Вписанный_тетраэдр.svg
[15] E.A. Power, T. Thirunamachandran, *Proc. R. Soc. Lond. A* **401**, 267 (1985).
[16] P.E. Argan, A. Piazzoli, *Phys. Lett.* **4**, 350 (1963).
[17] P.E. Argan *et al.*, *Phys. Rev. Lett.* **9**, 405 (1962).
[18] J.P. Schiffer, R. Vandenbosch, *Phys. Lett.* **5**, 292 (1963).
[19] F.M. Marqués *et al.*, *Phys. Rev. C* **65**, 044006 (2002).
[20] S.C. Pieper, *Phys. Rev. Lett.* **90**, 252501 (2003).
[21] K. Kisamori *et al.*, *Phys. Rev. Lett.* **116**, 052501 (2016).
[22] E. Hiyama, R. Lazauskas, J. Carbonell, M. Kamimura, *Phys. Rev. C* **93**, 044004 (2016).
[23] J. Carbonell, R. Lazauskas, E. Hiyama, M. Kamimura, *Few-Body Syst.* **58**, 67 (2017).
[24] R. Lazauskas, E. Hiyama, J. Carbonell, arXiv:1705.07927 [nucl-th].
[25] K. Fossez, J. Rotureau, N. Michel, M. Płoszajczak, *Phys. Rev. Lett.* **119**, 032501 (2017).